BMC Plant Biology

RESEARCH

Open Access

# Multi-combination comparative transcriptome analysis response to MeJA and identifies genes putatively involved in oridonin biosynthesis in *Isodon rubescens*

Conglong Lian[1,2,3†], Bao Zhang[1,2,3†], Fei Zhang[1,2], JinXu Lan[1,2], Jingfan Yang[1,2], Hao Yang[1,2], Jingjing Li[1,2] and Suiqing Chen[1,2,3,4*]

## Abstract

**Background** *Isodon rubescens*is used in traditional Chinese medicine and has drawn attention as a rich source of oridonin, a compound reported to possess medicinal properties. Differential transcriptome analysis is known to be an effective method for gene selection of diterpene oridonin biosynthetic pathways, however, the MeJA-induced genetic responses of *I. rubescens* have not yet been analyzed.

**Results** In this study, comparative transcriptome analysis of JY (with oridonin) and LS (no oridonin) lines of *I. rubescens* with or without a methyl jasmonate (MeJA) treatment revealed 43,115 assembled unigenes, 11,253 of which were differentially expressed. We also identified a total of 5,070 statistically significant differentially expressed unigenes which respond to MeJA including 397 transcription factor (TF) unigenes, such as bHLH, ERF, NAC, and MYB. Furthermore, assignments with KEGG pathways identified 18 of 53 unigenes referring to the diterpenoid biosynthesis, 10 cytochrome P450 unigenes, and three different expression TF unigenes were speculated that these genes could regulate the synthesis of oridonin based on MeJA induced. Finally, 18 unigenes were validated by qRT-PCR, and their expression levels were matched with the sequence data. In addition, Single Nucleotide Polymorphisms (SNPs) were analyzed and 14,609 simple sequence repeats (SSRs) were detected in *I. rubescens*, providing further support for future genetic variation and marker-assisted selection.

**Conclusions** This is the first time to study the response of related genes to MeJA treatment in *I. rubescens*, and some new genes were putatively involved in oridonin biosynthesis in *I. rubescens*. Our results provides a valuable gene resource to functionally characterize of response to MeJA and oridonin biosynthesis in *I. rubescens*.

**Keywords** Isodon rubescens, Transcriptome analysis, Oridonin biosynthesis, MeJA treatment, Transcription factor, SSR

†Conglong Lian and Bao Zhang contributed equally to this work.

*Correspondence:
Suiqing Chen
chsq@hactcm.edu.cn
[1]School of Pharmacy, Henan University of Chinese Medicine, 156 Esat Jin-shui Rd, Zhengzhou 450046, PR China
[2]Henan Key Laboratory of Chinese Medicine Resources and Chemistry, Zhengzhou 450046, PR China
[3]Collaborative Innovation Center of Research and Development on the Whole Industry Chain of Yu-Yao, Zhengzhou, Henan Province 450046, PR China
[4]Co-Construction Collaborative Innovation Centre for Chinese Medicine and Respiratory Diseases by Henan & Education Ministry of China, Zhengzhou 450046, PR China

## Background

Oridonin has received considerable attention as a compound with a range of pharmacological properties for the treatment of various diseases [1–5]. Oridonin has only been found in *Isodon rubescens* (Hemsley) H. Hara (*I. rubescens*), and the chemical structure of oridonin was elucidated by IR spectra, $^{1}$H-NMR and $^{13}$C-NMR.(Fig. 1) [6]. *I. rubescens* is classified in the tribe Ocimeae of the botanical family Lamiaceae and serves an important role in traditional Chinese medicine. It is officially listed in the *Chinese Pharmacopoeia* and is widely cultivated in Henan Province, China. In Chinese folk medicine, it is used to treat a wide variety of ailments and diseases [7]. There has been increased interest in exploring the oridonin biosynthesis pathway in *I. rubescens* due to its potential for high medicinal and commercial value.

Oridonin is a known ent-kauranoid diterpenoid, and until now its biosynthetic pathways have largely gone unstudied. Generally, the diterpene biosynthesis pathway in *I. rubescens* includes the upstream mevalonate (MVA) pathway (located in the cytosol) and the plastidial-located 2-C-methyl-D-erythritol-4-phosphate (MEP) pathway. These produce the C5 unit of isopentyl diphosphate (IPP) and dimethylallyl diphosphate (DMAPP). They also transform a midstream series of enzymes into different linear C5n prenyl diphosphates intermediates via processes including geranyl diphosphate synthase (GPPS), farnesyl diphosphate synthase (FPPS), and geranylgeranyl pyrophosphate synthase (GGPPS), which further form the carbocyclic skeleton of terpenoids [8, 9]. Furthermore, molecular characterizations of the genes involved in terpenoid biosynthesis have been intensively studied in many plant species, such as *Salvia miltiorrhiza* [10], *Artemisia annua* [11], and *Taxus chinensis* [12]. In the biosynthesis research of Oridonin in *I. rubescens*, excepts genes studied in the terpenoid backbone biosynthesis, IrCPS4 and IrCPS5 synthesize the intermediate ent-copalyl diphosphate (ent-CPP), and IrCYP706V2 and IrCYP706V7 oxidized the ent-kaurene core in the initial stage of oridonin biosynthesis [13, 14]. These previous studies lay a strong foundation, but it is clear that the biosynthetic pathway of oridonin in the *I. rubescens* requires further in-depth study.

RNA sequencing is a widely used technique that has recently been applied for the determination of gene expression patterns involved in the biosynthesis of secondary metabolites. This approach has proven to be an efficient and economical platform for gene discovery in non-model plants without knowing their genome sequences [15]. Hormones also play an important role in regulating plant growth and development during vital processes including seed germination, blossoming, root elongation, and stress response [16, 17]. Recent evidence has shown that the application of exogenous hormones can promote the yield of various plant secondary metabolites [18]. Methyl jasmonate (MeJA), one of the most important types of jasmonates (JAs), is a potent and important signaling molecule that regulates the production of multiple primary and secondary metabolites in plants. This compound is especially vital for the regulation of three major classes of plant secondary metabolites: terpenoids, alkaloids, and phenylpropanoids [17, 19]. So, considering how influential MeJA is on the synthesis of many different metabolites, transcript profiling together with metabolite analysis could prove valuable for the identification of genes in different metabolic pathways [20].

In this study, we explore oridonin biosynthesis and elucidate the mechanism of oridonin accumulation using two different lines of *I. rubescens* with or without MeJA treatments. Plants with significant differences in oridonin accumulation were then selected for RNA-sequencing and comparative transcriptome analysis.

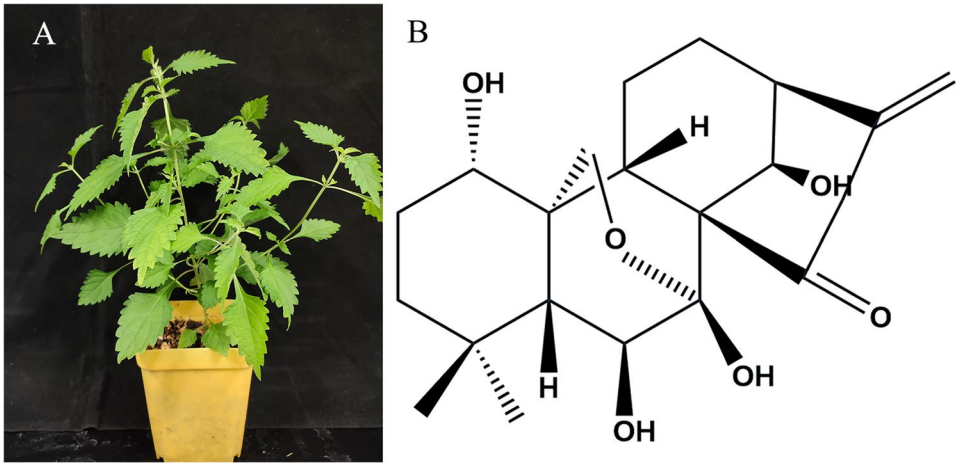


**Fig. 1** The plant pictures of *I. rubescens* (**A**) and the structure diagram of oridonin (**B**)

MeJA responses and candidate oridonin biosynthetic genes were then screened based on the expression differentially expressed gene of previously documented genes. Furthermore, quantitative real-time PCR (qRT-PCR) analysis supported the role of the candidate genes in oridonin biosynthesis. This comprehensive transcriptome analysis provides a basis for further research on enhancing oridonin biosynthesis in *I. rubescens*.

## Results

### Oridonin biosynthesis in *I. rubescens* was improved by MeJA stimuli

Exogenous stimuli were known to increase the secondary metabolite content in plants through signal transduction. This increase was especially large following the application of exogenous hormones, making it a powerful tool for the study of secondary metabolites [21]. In our study, compared to the controls, the MeJA treatment of JY lines caused significant changes in oridonin biosynthesis in the 3 h-, 12 h-, and 24 h-treated plants, but there was only a slight increase in the 6 h- treatment. The 3 h-treatment showed the highest increase in oridonin content, with improvements of 22.62% in the preliminary experiment (Fig. 2A). Based on these results the 3 h-treatment was selected as the method used for further tests on the JY and LS *I. rubescens* lines. As shown in Fig. 2B, JY lines had significant changes in oridonin biosynthesis caused by the MeJA 3 h-treatment. Oridonin content was not detected in LS lines with or without MeJA treatment (Fig. 2B). And the chromatograms of oridonin were also provided in Figure S1. This data suggests that MeJA could be an effective inducer for improving oridonin biosynthesis in *I. rubescens*.

### De novo assembly and functional annotation

The leaves of *I. rubescens* plants with (JY) and without (LS) oridonin were used to identify the response of transcriptomes to MeJA and genes putatively involved in oridonin biosynthesis. We constructed twelve cDNA libraries from three replicates of leaves with or without MeJA treatment. These libraries were named JY_M0h1, JY_M0h2, JY_M0h3, JY_M3h1, JY_M3h2, JY_M3h3, LS_M0h1, LS_M0h2, LS_M0h3, LS_M3h1, LS_M3h2, and LS_M3h3, and they were based on the 46.6 ~ 56.3 million raw reads we acquired using the Illumina Novaseq™ 6000 (LC Sciences, USA). All raw sequencing data had been deposited in the NCBI SRA database with the accession numbers SUB12343466. After processing and filtering out the contaminant sequences with poor-quality reads and adaptor sequences, more than 96.89% of the sequencing reads were valid with good values of Q20, Q30, and GC content (Table 1). In total, 148,584 transcripts containing 43,115 unique genes were obtained from all twelve transcriptomes (Table 2). These results suggest that the qualities of these assemblies are highly reliable for further bioinformatics analyses.

For sequence annotation, all 43,115 assembled unigenes were aligned against the non-redundant (Nr) protein database, Gene ontology (GO), SwissProt, Pfam, Kyoto Encyclopedia of Genes and Genomes (KEGG), and eggNOG databases using DIAMOND with a threshold of Evalue < 0.00001. A sum of 22,736 unigenes (52.73%) were annotated using the GO database and categorized into three main GO domains—biological processes (19,038 unigenes, 44.16%), cellular components (20,217 unigenes, 46.89%), and molecular function (19,818 unigenes, 45.97%) (Table S2). Furthermore, 43,115 annotated unigenes were aligned against the KEGG database and 18,344 unigenes (42.55%) were mapped to 141 KEGG

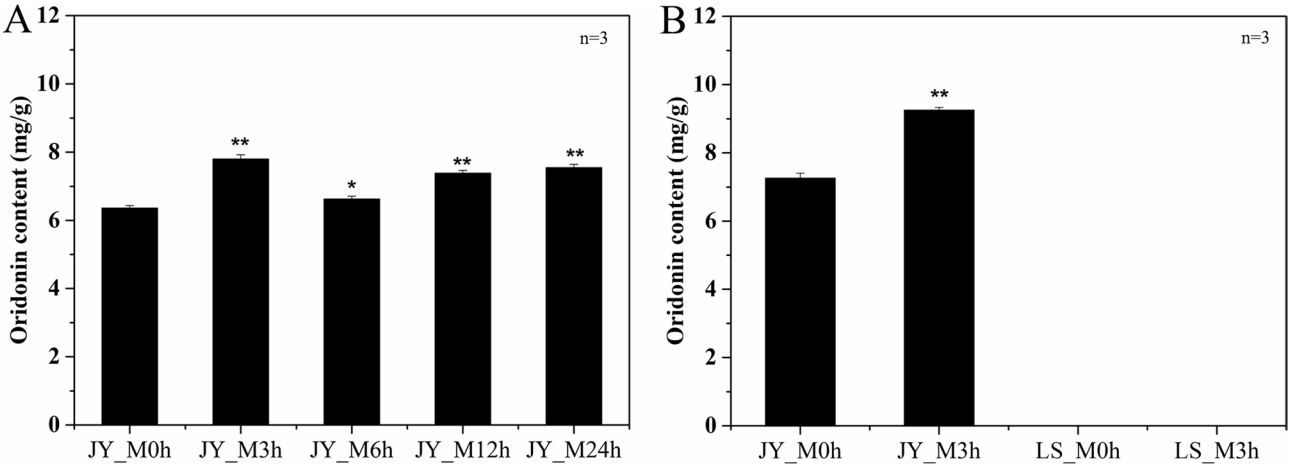


**Fig. 2** The oridonin content in different lines of *I. rubescens* under MeJA treatment. **A** The *I. rubescens* of JY lines under various MeJA treatment times. **B** The *I. rubescens* of JY and LS lines under MeJA treatment. Error bars indicate ± SD of three biological replicates and tested by paired Student's t test. The mark "**" indicate very significant difference ($p < 0.01$) relative to the corresponding control JY_M0h at each time point

**Table 1** Summary of the sequencing data of the transcriptomes of *I. rubescens*

| Sample | Raw Reads | Raw Bases | Valid Reads | Valid Bases | Valid% | Q20% | Q30% | GC% |
|---|---|---|---|---|---|---|---|---|
| JY_M0h1 | 49,971,500 | 7.50G | 48,977,398 | 6.86G | 98.01 | 98.31 | 94.38 | 47.96 |
| JY_M0h2 | 50,326,752 | 7.55G | 49,017,108 | 6.86G | 97.40 | 98.32 | 94.36 | 47.37 |
| JY_M0h3 | 53,389,566 | 8.01G | 51,885,496 | 7.27G | 97.18 | 98.38 | 94.56 | 48.49 |
| JY_M3h1 | 49,376,198 | 7.41G | 48,011,168 | 6.72G | 97.24 | 98.33 | 94.44 | 47.35 |
| JY_M3h2 | 52,987,468 | 7.95G | 51,540,844 | 7.22G | 97.27 | 98.33 | 94.42 | 47.60 |
| JY_M3h3 | 48,564,068 | 7.28G | 47,583,432 | 6.66G | 97.98 | 98.35 | 94.50 | 47.55 |
| LS_M0h1 | 46,713,474 | 7.01G | 45,505,146 | 6.38G | 97.41 | 98.41 | 94.65 | 49.05 |
| LS_M0h2 | 48,229,232 | 7.23G | 46,728,422 | 6.54G | 96.89 | 98.35 | 94.45 | 47.51 |
| LS_M0h3 | 55,082,514 | 8.26G | 53,510,714 | 7.49G | 97.15 | 98.34 | 94.48 | 47.14 |
| LS_M3h1 | 50,536,508 | 7.58G | 49,563,640 | 6.94G | 98.07 | 98.37 | 94.55 | 47.25 |
| LS_M3h2 | 56,295,298 | 8.44G | 55,241,864 | 7.74G | 98.13 | 98.40 | 94.59 | 47.28 |
| LS_M3h3 | 46,628,612 | 6.99G | 45,373,248 | 6.35G | 97.31 | 98.35 | 94.47 | 47.12 |

**Table 2** Summary of annotations of the *I. rubescens* unigenes

| Annotated in databases | Number of Genes | Ratio (%) |
|---|---|---|
| All transcript | 148,584 | |
| All annotated | 43,115 | 100.00 |
| Annotated in GO | 22,736 | 52.73 |
| Annotated in KEGG | 18,344 | 42.55 |
| Annotated in Pfam | 21,156 | 49.07 |
| Annotated in swissprot | 19,044 | 44.17 |
| Annotated in eggNOG | 25,385 | 58.88 |
| Annotated in NR | 26,735 | 62.01 |

pathways. These unigenes were then categorized into six main domains of KEGG Level1—metabolism (5,346 unigenes), genetic information processing (2,719 unigenes), environmental information processing (1,014 unigenes), organismal systems (1,520 unigenes), cellular processes (598 unigenes), and human diseases (53 unigenes). Based upon the number of unigenes assigned, carbohydrate metabolism (1,253 unigenes), amino acid metabolism (678 unigenes), and lipid metabolism (633 unigenes) are the dominant metabolic pathways, and signal transduction (889) is the dominant environmental information processing pathways (Figure S2). Additionally, 21,156 (49.07%), 19,044 (44.17%), 25,385 (58.88%), and 26,735 (62.013%) unigenes were annotated using the Pfam, Swissprot, eggNOG, and NR databases, respectively (Table 2).

### Identification of differential expression genes (DEGs) involved in MeJA treatment

A total of 5,070 of 11,253 statistically significant differentially expressed genes (DEGs) were identified as being responsive to the presence of MeJA. DEGs were determined based on the criteria of |log2 Fold Change| ≥ 1, with a p-value ≤ 0.05. 3,197 of these DEGs were identified in JY response to MeJA in which 1,750 unigenes were up-regulated and the remaining 1,447 were down-regulated (Fig. 3A, Table S3). The other 2,251 DEGs were identified in LS response to MeJA in LS_M3h_vs_LS_M0h, in which 1251 unigenes were up-regulated and the remaining 1,300 were down-regulated (Fig. 3A, Table S4). Comprehensive analysis showed that only 222 up-regulated (Fig. 3B) and 156 down-regulated (Fig. 3C) unigenes were a concordant response to MeJA in the JY and LS lines, suggesting that the pattern of gene expression differs greatly between lines.

GO and KEGG enrichment analyses were conducted to further explore the possible role of these DEGs. During a

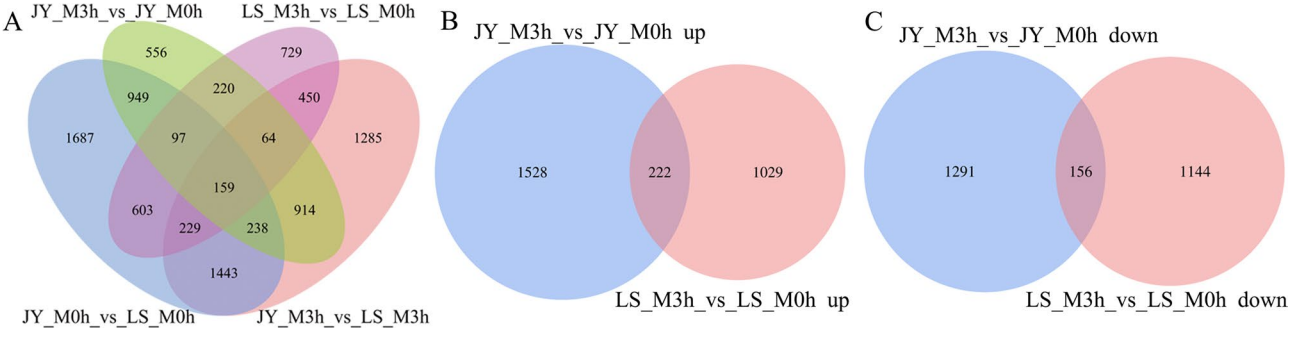


**Fig. 3** Venn diagram analysis of differential expression genes. **A** Venn diagram analysis of different expression genes identified response to MeJA. **B** Venn comprehensive analysis of up-regulated genes in JY_M3h_vs_JY_M0h and LS_M3h_vs_LS_M0h, **C** Venn comprehensive analysis of down-regulated genes in JY_M3h_vs_JY_M0h and LS_M3h_vs_LS_M0h

comparison of the JY lines with or without MeJA treatment of JY_M3h vs. JY_M0h, 1,772 DEGs were annotated to the GO pathway. A majority of the unigenes were assigned to biological processes (3,305 unigenes), followed by molecular functions (3,010 unigenes), and cellular components (2,733 unigenes). The most common GO terms within biological processes included defense response (179 unigenes, GO:0006952), protein phosphorylation (134 unigenes, GO:0006468), and biological processes (132, GO:0008150). In the cellular component class, the largest three categories were plasma membrane (395, GO:0005886), nucleus (321 unigenes, GO:0005634), and integral components of the membrane (321 unigenes, GO:0016021). In the molecular function category, the classes related to ATP binding (223 unigenes, GO:0005524), protein serine/threonine kinase activity (193 unigenes, GO:0004674), and protein binding (149 unigenes, GO:0005515) were the most frequently observed (Fig. 4A). During the comparison of the LS lines of LS_M3h vs. LS_M0h, 1561 significant unigenes were annotated to the GO pathway. A majority of the unigenes were assigned to biological processes (3,248 unigenes), followed by molecular functions (2,691 unigenes), and cellular components (2,477 unigenes). The most common GO terms within biological processes, molecular function, and cellular components were similar to JY lines (Fig. 4B). These results indicate that MeJA mainly regulates the growth and development of *I. rubescens* through these GO terms.

A total of 1,590 DEGs could be mapped to 119 pathways of the KEGG database. The KEGG analysis results of DEGs annotation for both JYs and LSs lines with or without MeJA treatment showed that the KEGG pathways were commonly associated with flavonoid biosynthesis, isoquinoline alkaloid biosynthesis, phenylalanine metabolism, phenylpropanoid biosynthesis, photosynthesis, plant-pathogen interaction, sesquiterpenoid and triterpenoid biosynthesis, and tyrosine metabolism with the p value ≤ 0.05 (Fig. 5A, B). All of these pathways (except tyrosine metabolism) are involved in the biosynthesis of secondary metabolites, indicating that MeJA mainly regulates the secondary metabolism of *I. rubescens*. Furthermore, terpenoids were known to be the main active constituents of *I. rubescens* [1]. 11 and 8 DEGs were mapped to the diterpenoid biosynthesis pathway of the JYs (p-value 0.05) and LSs (p-value 0.18), respectively (Table 3).

### Identification of DEGs involved in two different lines of *I. rubescens*

A total of 5405 (2426 up-regulated and 2979 down-regulated) and 4782 (2364 up-regulated and 2418 down-regulated) statistically significant differentially expressed genes (DEGs) were identified in comparison of JY_M0h_vs_LS_M0h and JY_M3h_vs_LS_M3h, respectively. For the DEGs of JY_M0h_vs_LS_M0h, the KEGG analysis results showed that the KEGG pathways were commonly associated with Plant-pathogen interaction, Phenylpropanoid biosynthesis, MAPK signaling pathway - plant, Stilbenoid, diarylheptanoid and gingerol biosynthesis, Isoquinoline alkaloid biosynthesis, Flavonoid biosynthesis, Tyrosine metabolism, Cutin, suberine and wax biosynthesis, Cyanoamino acid metabolism, and Indole alkaloid biosynthesis with the p value ≤ 0.005 (Fig. 5C). For the DEGs of JY_M3h_vs_LS_M3h, the KEGG analysis results showed that the KEGG pathways were commonly associated with Plant-pathogen interaction, Phenylpropanoid biosynthesis, Isoquinoline alkaloid biosynthesis, Phenylalanine metabolism, RNA polymerase, Galactose metabolism, Flavonoid biosynthesis, Stilbenoid, diarylheptanoid and gingerol biosynthesis, Tyrosine metabolism, MAPK signaling pathway - plant, Brassinosteroid biosynthesis, Diterpenoid biosynthesis, Tryptophan metabolism, and Cyanoamino acid metabolism with the p value ≤ 0.005 (Fig. 5D). Furthermore, 2069 gene were common DEGs of JY_M0h_vs_LS_M0h and JY_M3h_vs_LS_M3h, and 173 genes were particularly related to expressed in JY lines that are not or extremely low expressed with the mean_TPM ≤ 0.5 in LS lines (Table S5). Among them, two genes, including TRINITY_DN19681_c0_g1 (nezukol synthase, SBS) and TRINITY_DN15337_c0_g4 (ent-kaurene synthase, KS), in the diterpenoid biosynthesis pathway were particularly speculated to be related to oridonin biosynthesis.

### Identification of unigenes involved in secondary metabolism

KEGG pathway analysis indicated that the majority of unigenes (5,346 of 18,344 KEGG annotation unigenes) were annotated to the metabolism category. For the MeJA treatment, KEGG pathway annotation of DEGs showed that MeJA mainly regulates secondary metabolism in *I. rubescens*. Our study identified many unigenes, especially DEGs, involved in secondary metabolism. The number of unigenes related to different secondary metabolic processes is listed in Table 3. Out of all analyzed unigenes involved in secondary metabolite pathways, those involved with "phenylpropanoid biosynthesis (ko00940, 276 unigenes)" had the highest proportion, followed by "flavonoid biosynthesis (ko00941, 127 unigenes)", "stilbenoid, diarylheptanoid, and gingerol biosynthesis (ko00945, 89 unigenes)", and "terpenoid backbone biosynthesis (ko00900, 83 unigenes)". Table 3 shows that most of the synthesis genes in the metabolite pathways were up-regulated by MeJA, such as ubiquinone and other terpenoid-quinone biosynthesis, terpenoid backbone biosynthesis, and carotenoid biosynthesis (Table 3). Surprisingly, analysis of the diterpenoid pathway revealed

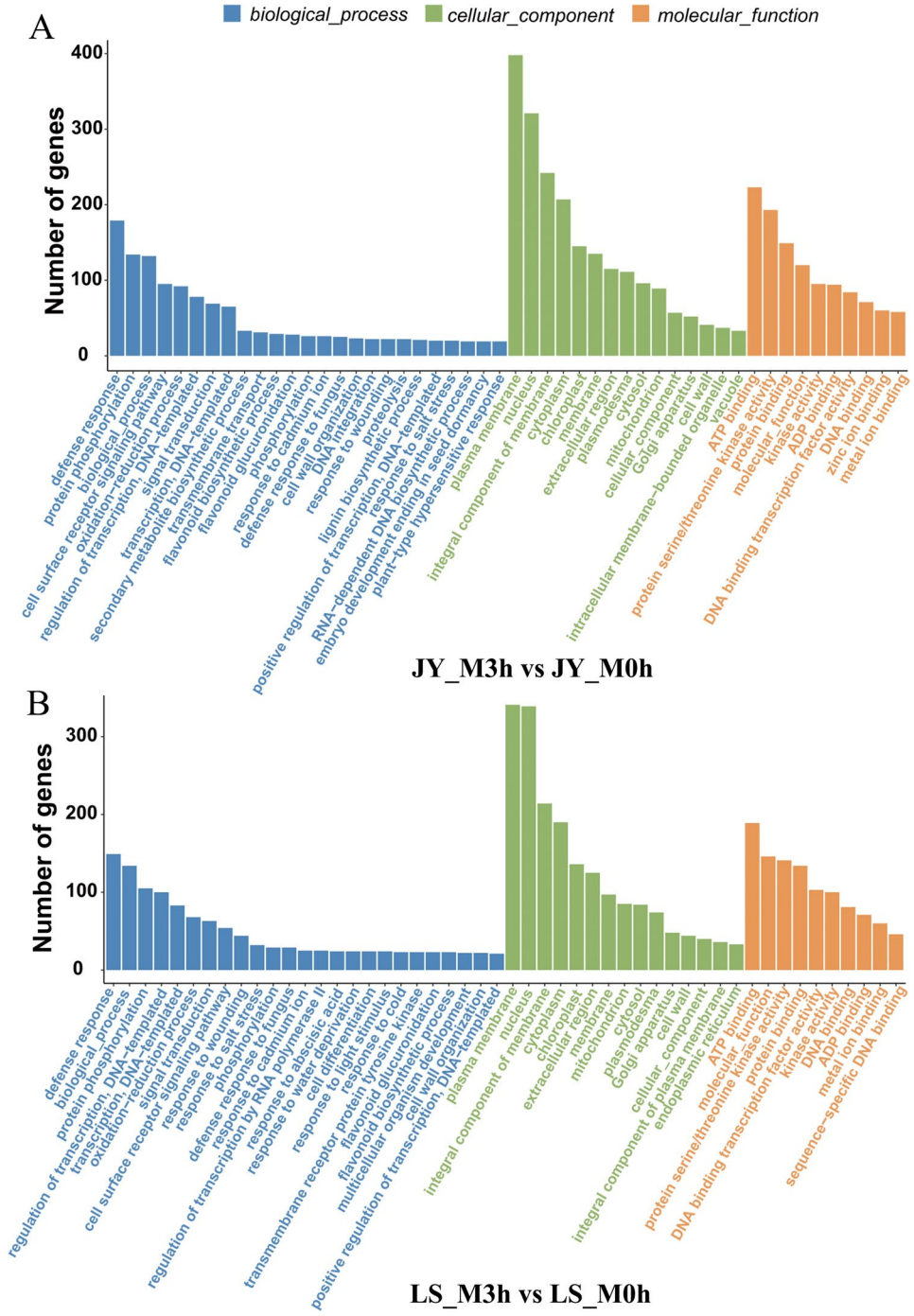


**Fig. 4** Gene ontology (GO) classification analysis of the MeJA response DEGs in *I. rubescens*. **A** JY_M3h vs. JY_M0h, **B** LS_M3h vs. LS_M0h. The Y-axis shows the gene numbers for each different term

that most genes of terpenoid backbone biosynthesis were up-regulated, including 6 of 7 genes, and 8 of 9 genes significant up-regulated in JY_M3h vs. JY_M0h, and LS_M3h vs. LS_M0h, respectively. while more genes in the diterpenoid biosynthesis were down-regulated, including 7 of 11 genes, and 5 of 8 genes significant down-regulated in JY_M3h vs. JY_M0h, and LS_M3h vs. LS_M0h, respectively (Table 3). Furthermore, for the two lines of *I. rubescens*, comparison of the differential genes in the relevant secondary metabolism regulatory pathways of JY and LS lines revealed that there were also exsit several DEGs, indicating that there were some differences in the synthesis of secondary metabolites between the two lines (Table 3). Among them, 13 and 13 DEGs were present

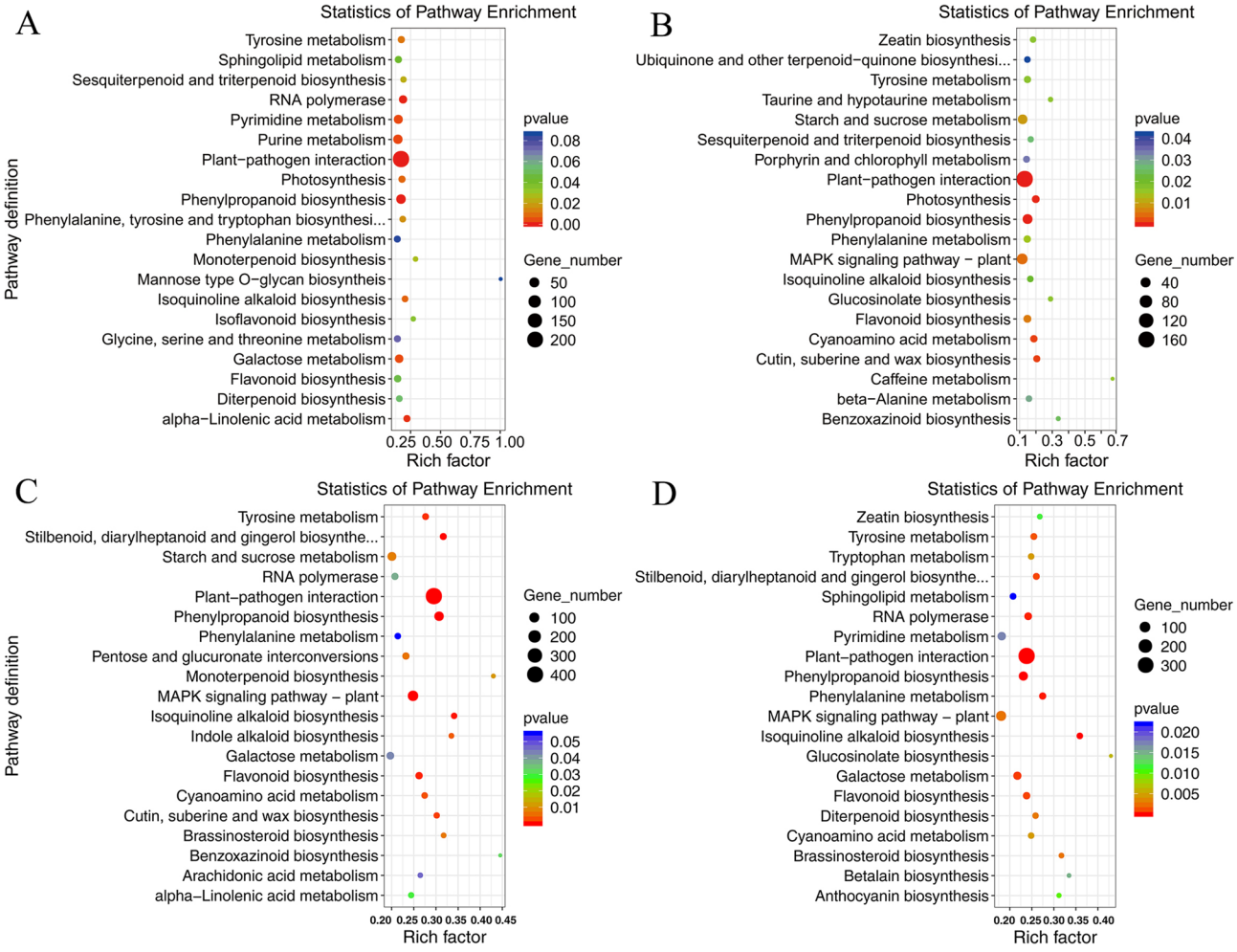


**Fig. 5** Statistics of DEGs KEGG pathway enrichment for two lines of *I. rubescens* with or without MeJA treatment. Distribution of the differentially expressed genes obtained from the comparative analysis of JY_M0h and JY_M3h of JY lines (**A**), LS_M0h and LS_M3h of LS lines (**B**), JY_M0h and LS_M0h (**C**), and JY_M3h and JY_M3h (**D**). The Y-axis on the right side represents the number of genes

in the comparison of JY_M0h vs. LS_M0h and JY_M3h vs. LS_M3h in the diterpenoid backbone biosynthesis pathway, respectively. In the diterpenoid biosynthesis pathway, there were 14 and 19 DEGs in the comparison of JY_M0h vs. LS_M0h and JY_M3h vs. LS_M3h, respectively (Table 3). In addition, the KEGG diagram of terpene backbone, monoterpene, diterpene, sesquiterpenoid and triterpenoi, ubiquinone and other terpenoid biosynthetic pathway related to the differential genes were also annotated in Supplementary Table S6.

### Identification of genes related to Oridonin biosynthesis

Prior to treatment, oridonin was already known to accumulate in JY lines and not LS lines and following the MeJA treatment, there was a significant oridonin increase only in JY lines. JY_M3h vs. JY_M0h, JY_M0h vs. LS_M0h, and JY_M3h vs. LS_M3h were comparatively analyzed (Fig. 6A). As shown in Fig. 5A, there were 776 DEGs expressed specifically in JY_M3h vs. JY_M0h (Fig. 6A, Table S7). It is speculated that these genes may be involved in regulating the synthesis of oridonin. The superfamily of cytochrome P450 (CYP450) enzymes plays a key role in plant evolution and metabolic diversification. These enzymes are essential for the biosynthesis of secondary metabolites and terpenoids in plants. We found ten cytochrome P450 genes in the 776 DEGs: TRINITY_DN11269_c0_g3 (*CYP94A1*), TRINITY_DN11322_c0_g1 (*CYP76C1-like*), RINITY_DN11322_c0_g2 (*CYP76C1-like*), TRINITY_DN13891_c0_g5 (*CYP72A68-like*), TRINITY_DN15791_c0_g3 (*CYP81E8-like*), TRINITY_DN19470_c0_g1 (*CYP94C54*), TRINITY_DN19470_c0_g2 (*CYP94C1*), TRINITY_DN20257_c1_g3 (*CYP72A294*), TRINITY_DN21332_c1_g2 (*CYP76C1-like*), and TRINITY_DN21572_c1_g3 (*CYP84A60*).

Furthermore, the genes mapped to terpenoid backbone biosynthesis (map00900, 83 genes) and diterpenoid biosynthesis (map00904, 74 genes) of KEGG pathways may be involved in the regulation of oridonin biosynthesis were also

**Table 3** Numbers of unigene related to the secondary metabolism biosynthesis pathway in *I. rubescens*

| Secondary Metabolites Biosynthesis Pathway | Total mapped genes | JY_M3h vs. JY_M0h | | | LS_M3h vs. LS_M0h | | | JY_M0h vs. LS_M0h | | | JY_M3h vs. LS_M3h | | |
|---|---|---|---|---|---|---|---|---|---|---|---|---|---|
| | | Sig. | Up | Down | Sig | Up | Down | Sig. | Up | Down | Sig. | Up | Down |
| Steroid biosynthesis (map00100) | 33 | 1 | 1 | 0 | 3 | 2 | 1 | 3 | 2 | 1 | 5 | 4 | 1 |
| Ubiquinone and other terpenoid-quinone biosynthesis (map00130) | 63 | 6 | 6 | 0 | 9 | 8 | 1 | 11 | 5 | 6 | 13 | 9 | 4 |
| Terpenoid backbone biosynthesis (map00900) | 83 | 7 | 6 | 1 | 9 | 8 | 1 | 13 | 7 | 6 | 13 | 6 | 7 |
| Indole alkaloid biosynthesis (map00901) | 36 | 5 | 1 | 4 | 6 | 3 | 3 | 12 | 5 | 7 | 9 | 3 | 6 |
| Monoterpenoid biosynthesis (map00902) | 14 | 4 | 2 | 2 | 1 | 1 | 0 | 6 | 5 | 1 | 3 | 3 | 0 |
| Limonene and pinene degradation (map00903) | 9 | 2 | 1 | 1 | 1 | 1 | 0 | 1 | 1 | 0 | 1 | 1 | 0 |
| Diterpenoid biosynthesis (map00904) | 74 | 11 | 4 | 7 | 8 | 3 | 5 | 14 | 12 | 2 | 19 | 10 | 9 |
| Brassinosteroid biosynthesis (map00905) | 38 | 5 | 0 | 5 | 3 | 0 | 3 | 12 | 2 | 10 | 12 | 2 | 10 |
| Carotenoid biosynthesis (map00906) | 74 | 10 | 9 | 1 | 8 | 6 | 2 | 15 | 11 | 4 | 13 | 6 | 7 |
| Zeatin biosynthesis (map00908) | 45 | 4 | 3 | 1 | 8 | 5 | 3 | 8 | 4 | 4 | 12 | 5 | 7 |
| Sesquiterpenoid and triterpenoid biosynthesis (map00909) | 49 | 9 | 8 | 1 | 8 | 4 | 4 | 10 | 2 | 8 | 10 | 3 | 7 |
| Phenylpropanoid biosynthesis (map00940) | 276 | 44 | 25 | 19 | 39 | 27 | 12 | 84 | 51 | 33 | 63 | 43 | 20 |
| Flavonoid biosynthesis (map00941) | 127 | 17 | 11 | 6 | 18 | 13 | 5 | 35 | 15 | 20 | 34 | 17 | 17 |
| Anthocyanin biosynthesis (map00942) | 29 | 5 | 4 | 1 | 4 | 4 | 0 | 7 | 1 | 6 | 9 | 3 | 6 |
| Isoflavonoid biosynthesis (map00943) | 15 | 4 | 4 | 0 | 2 | 2 | 0 | 2 | 0 | 2 | 4 | 1 | 3 |
| Stilbenoid, diarylheptanoid, and gingerol biosynthesis (map00945) | 89 | 9 | 6 | 3 | 11 | 6 | 5 | 28 | 9 | 19 | 23 | 13 | 10 |
| Isoquinoline alkaloid biosynthesis (map00950) | 56 | 11 | 8 | 3 | 9 | 5 | 4 | 19 | 13 | 6 | 20 | 15 | 5 |
| Tropane, piperidine and pyridine alkaloid biosynthesis (map00960) | 29 | 4 | 4 | 0 | 3 | 1 | 2 | 5 | 2 | 3 | 5 | 5 | 0 |
| Betalain biosynthesis (map00965) | 21 | 2 | 0 | 2 | 4 | 1 | 3 | 6 | 2 | 4 | 7 | 2 | 5 |
| Glucosinolate biosynthesis (map00966) | 14 | 1 | 1 | 0 | 4 | 3 | 1 | 4 | 3 | 1 | 6 | 5 | 1 |

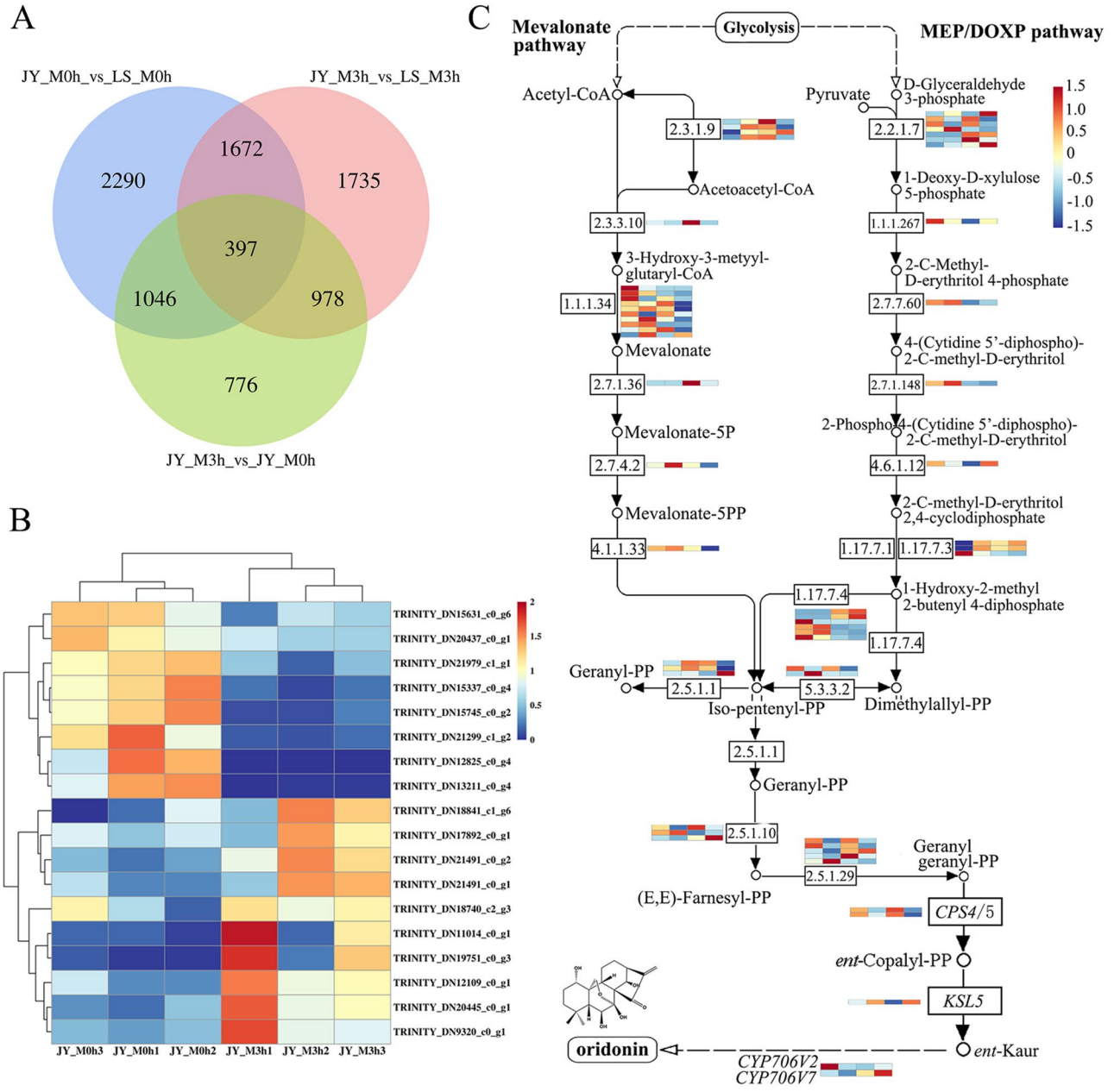


**Fig. 6** Genes related to oridonin biosynthesis. **A** Venn diagram analysis of DEGs of JY_M3h vs. JY_M0h, JY_M0h vs. LS_M0h, and JY_M3h vs. LS_M3h. **B** The heatmap analysis of DEGs in the terpenoid biosynthesis pathway for the JY_M3h vs. JY_M0h. The data were normalized by standardization. **C** The biosynthesis pathway of oridonin along side with the mean_TPM expression of genes, the heatmap from left to right is JY_M3h, _JY_M0h, LS_M3h, and LS_M0h. The data were normalized by Z-score

analyzed (Table S8). They were 157 genes mapped, among these genes, the expression analysis showed 53 were DEGs. Based on the response of oridonin to MeJA in JY lines, a heatmap of DEGs in the terpenoid biosynthesis pathway for the JY_M3h vs. JY_M0h was made. 18 genes showed a significant response to MeJA in the biosynthesis pathway of terpenoid compounds, including 3-hydroxy-3-methylglutaryl-coenzyme A reductase 3 (TRINITY_DN17892_c0_g1), kaurene synthase 4 (TRINITY_DN21979_c1_g1), ent-kaurene synthase (TRINITY_DN15745_c0_g2), and cytochrome P450 CYP82U4 (TRINITY_DN20437_c0_g1) (Fig. 6B). Among them, 12 showed a significant up-regulated by MeJA of JY lines, including TRINITY_DN19751_c0_g3 (ISPH), TRINITY_DN11014_c0_g1 (GGR), TRINITY_DN20445_c0_g1 (DAO), TRINITY_DN21491_c0_g2 (HMG2), TRINITY_DN18841_c1_g6 (LOC108838220), TRINITY_DN11322_c0_g1 (IrCYP706V2), TRINITY_DN21217_c0_g1 (IrCYP706V7), TRINITY_DN21491_c0_g1 (HMG), TRINITY_DN12109_c0_g1 (T6ODM), TRINITY_DN9320_c0_g1 (AOP1.2), TRINITY_DN18740_c2_g3 (DHDDS), and

TRINITY_DN17892_c0_g1(HMGR) (Fig. 6B). It is speculated that these genes can regulate the synthesis of oridonin based on MeJA induction.

In addition, base on the previous reports that tandem-duplicated CYP706V oxidase genes control oridonin biosynthesis [15], *IrCYP706V2* and *IrCYP706V7* genes expression were also analysised. It can seem that the expression *IrCYP706V2* and *IrCYP706V7* genes were also significant induced by MeJA, and these results were consistent with MeJA treatment to increase the content of oridonin (Fig. 2). Above all, the putatively biosynthesis pathway of oridonin alongside with the mean_TPM expression of genes were constructed (Fig. 6C, Table S9).

### Transcription factors predicted

Previous research has shown that transcription factors (TFs) of AP2/ERF, bHLH, WRKY, and MYB are involved in regulating the biosynthesis of terpenoids [22]. Based on this, it is possible that MeJA-induced TFs may be involved in the regulation of terpenoid biosynthesis. A total of 1,433 unigenes were annotated as TFs based on the reference of *Salvia miltiorrhiza* transcription factors in the PlantTFDB (http://planttfdb.gao-lab.org/index.php? sp=Smi). They were grouped into 48 families such as bHLH, ERF, Trihelix, NAC, and MYB (Fig. 7, Table S10). The bHLH transcription factor family was the largest, with 564 members accounting for 39% of the total TFs (Fig. 7A). Out of the 1,433 TF unigenes, 397 had differential expression in the comparison of JY_M3h vs. JY_M0h vs. LS_M3h vs. LS_M0h. 117 and 105 TF unigenes demonstrated DEGs in response to the MeJA treatment of JY_M3h vs. JY_M0h and LS_M3h vs. LS_M0h, respectively. The bHLH, ERF, NAC, and bZIP families were the most abundant of these MeJA-regulated TFs. Furthermore, based on the difference in oridonin content, 53 differentially expressed TF unigenes were found in both the comparison groups of JY_M0h vs. LS_M0h and JY_M3h vs. LS_M3h. Only 3 of the same differentially expressed TF unigenes were noted in the comparison groups of JY_M3h vs. JY_M0h, JY_M0h vs. LS_M0h, and JY_M3h vs. LS_M3h, including TRINITY_DN10953_c0_g1 (GRAS), TRINITY_DN19246_c0_g3 (ERF), and TRINITY_DN17215_c0_g2 (WRKY) (Fig. 7B). These results constitute a valuable TF gene resource for further studies of the regulatory functions in oridonin biosynthesis.

## RT-qPCR validation of differential gene expression

RNA sequencing was used to verify the credibility of the gene expression data of JY and LS lines with or without MeJA treatments. Eighteen unigenes were randomly selected for real-time PCR analysis, including four differential genes in the diterpenoid biosynthesis pathway (*HMGR*, *HMGR1*, *GGR*, and *ISPG*), and three differential genes in the terpenoid backbone biosynthesis pathway (*GA2*, *AOP1.2*, and *KSL4*). As shown in Fig. 7, RT-qPCR gene expression profiling matched well with data obtained from the RNA-sequencing expression profiling, suggesting that our differential expression data is reliable (Fig. 8).

### Statistics of single nucleotide polymorphisms and simple sequence repeats

Molecular markers are widely used for candidate gene and QTL identification through linkage or association mapping as well as analysis of population structure and evolution [23]. SNPs (Single Nucleotide

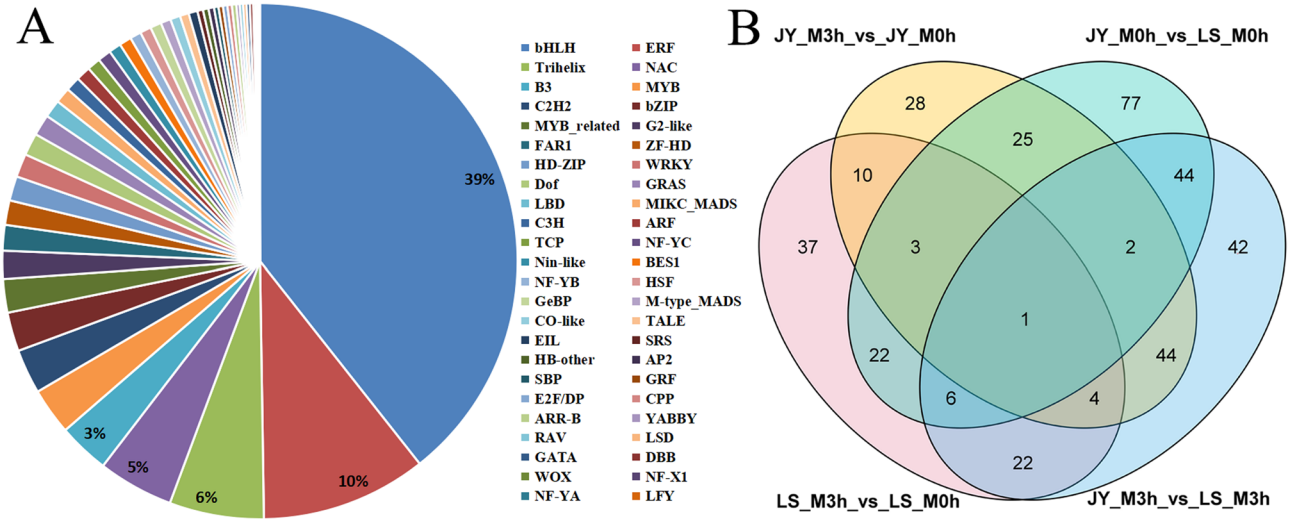


**Fig. 7** Transcription factors predicted. **A** Fan chart of the number of transcription factor family members. **B** Venn diagram analysis of transcription factors in comparison groups JY_M3h vs. JY_M0h, LS_M3h vs. LS_M0h, JY_M0h vs. LS_M0h, and JY_M3h vs. LS_M3h

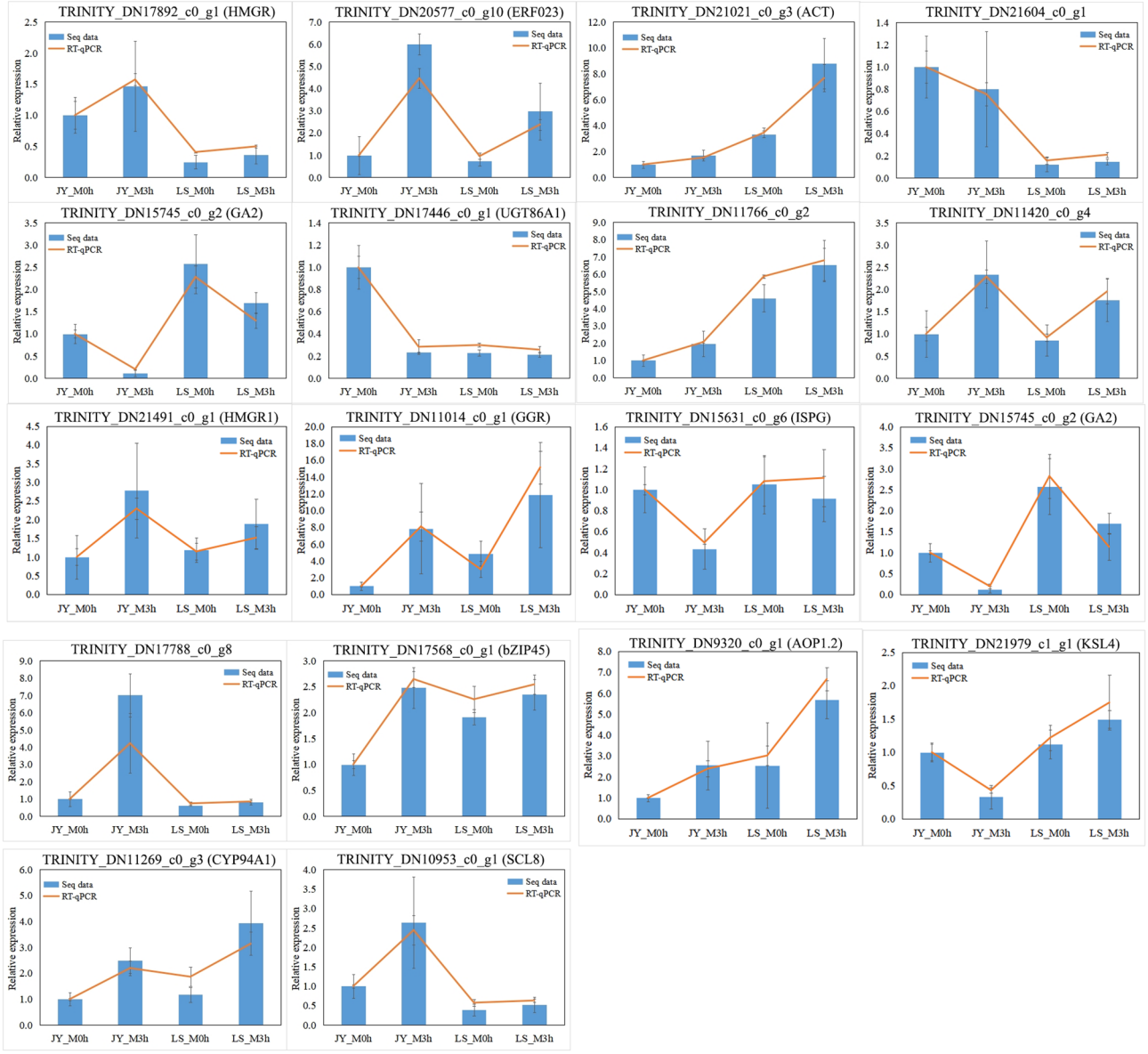


**Fig. 8** Real-time PCR validation analysis of twelve unigenes in the two lines of *I. rubescens* with or without MeJA treatment. RT-qPCR results presented by mean value of triplicate ± SE. Sequence data is based on normalization to 1 of JY_M0h_mean_TPM, and the other groups are based on the multiples of JY_M0h_mean_TPM

Polymorphism) are currently the genetic markers of choice since they are virtually unlimited, evenly distributed along the genome, bi-allelic, and co-dominant [24]. Previous studies have shown that SNPs can be divided into transition (C-T, on its complementary chain, A-G) and transversion (A-C, A-T, C-G, G-T), and the incidence of transition is always significantly higher than that of other variants. In our study, the total SNPs in each library ranged from 65,862 ~ 106,465, and the incidence of transition (38,898 ~ 63,299) was significantly higher than that of transversion (26,964 ~ 43,054) in each library (Table 4). Furthermore, more total SNPs in JY libraries were more than in LS libraries, and similar results were found for the total numbers of transitions and transversions (Table 4). In summary, these results indicate that JY lines have more polymorphic loci than LS lines.

Simple sequence repeats (SSRs) are one of the most important molecular markers and have various applications in genetics and plant breeding [25]. Thus, SSRs in *I. rubescens* were analyzed in our present study. A total of 14,609 SSRs were identified (Table S11) and of that di-nucleotide repeats (5,858) were the most abundant, followed by mononucleotide repeats (4,895),

**Table 4** Numbers of single nucleotide polymorphisms in *I. rubescens* libraries

| SNP type | JY M0h1 | JY M0h2 | JY M0h3 | JY M3h1 | JY M3h2 | JY M3h3 | LS M0h1 | LS M0h2 | LS M0h3 | LS M3h1 | LS M3h2 | LS M3h3 |
|---|---|---|---|---|---|---|---|---|---|---|---|---|
| Transition | 53,740 | 57,337 | 63,299 | 52,983 | 54,537 | 63,111 | 38,898 | 57,220 | 58,682 | 49,216 | 62,770 | 47,575 |
| A-G | 26,432 | 28,334 | 31,145 | 26,059 | 26,874 | 31,084 | 19,136 | 28,332 | 29,168 | 24,312 | 31,175 | 23,630 |
| C-T | 27,308 | 29,003 | 32,154 | 26,924 | 27,663 | 32,027 | 19,762 | 28,888 | 29,514 | 24,904 | 31,595 | 23,945 |
| Transversion | 36,408 | 38,698 | 42,213 | 36,822 | 37,288 | 43,054 | 26,964 | 39,413 | 40,970 | 33,904 | 42,927 | 32,943 |
| A-C | 8828 | 9437 | 10,182 | 8969 | 9057 | 10,494 | 6556 | 9670 | 10,021 | 8277 | 10,449 | 8038 |
| A-T | 10,151 | 10,822 | 11,729 | 10,302 | 10,527 | 12,002 | 7579 | 10,922 | 11,364 | 9470 | 11,890 | 9235 |
| C-G | 8620 | 9057 | 9936 | 8677 | 8665 | 10,093 | 6362 | 9279 | 9735 | 7927 | 10,126 | 7695 |
| G-T | 8809 | 9382 | 10,366 | 8874 | 9039 | 10,465 | 6467 | 9542 | 9850 | 8230 | 10,462 | 7975 |
| Total | 90,148 | 96,035 | 105,512 | 89,805 | 91,825 | 106,165 | 65,862 | 96,633 | 99,652 | 83,120 | 105,697 | 80,518 |

tri-nucleotide repeats (2,337), and compound SSRs (1340), penta-nucleotide repeats were the least ubiquitous (25) (Fig. 9).

## Discussion

Comparative transcriptome analysis has been successfully applied to the identification of genes involved in several secondary metabolic activities [15]. Jasmonates, including jasmonic acid (JA) and its methyl ester (MeJA), have been confirmed as effective elicitors for boosting the biosynthesis of many highly valuable and pharmaceutical secondary metabolites in various medicinal plants [17]. Previous studies have shown that many secondary metabolites can be induced by MeJA, including terpenoids, carotenoids, volatile, flavonoids, unsaturated fatty acids, and lycopene [26, 27]. Although efforts have been made to understand the role of hormones in plant metabolism, the detailed mechanisms remain unclear. In this study, the biosynthesis of oridonin, the main active ingredient of *I. rubescens*, was induced by MeJA (Fig. 1). High-throughput sequencing technologies were used to create an extensive analysis of *I. rubscences* transcriptomes by identifying putative genes involved in MeJA response and oridonin biosynthesis. These transcriptomes were derived from the leaves of two different lines (JY and LS) with and without MeJA treatment. Investigation of transcriptomes provides evidence for the role of MeJA in inducing secondary metabolism. Similar research has been conducted in other plants, such as *Polygonum minus* [28], *Panax quinquefolius* [29], *Centella asiatica* [30], and *Salvia miltiorrhiza* Bunge [31].

Since oridonin accumulates in JY lines and not LS lines, the rationale for screening genes involved in oridonin biosynthesis was based on choosing candidate genes that would be JY lines-dependently expressed and differentially expressed between JY and LS lines. Our study revealed that oridonin accumulation was significantly increased with MeJA treatment in JY lines. Thus, comparative transcriptome analysis was performed between JY vs. LS and JY_M3h vs. JY_M0h. There were 776 DEGs expressed specifically in JY_M3h vs. JY_M0h. And 157 genes were mapped to terpenoid backbone biosynthesis (map00900, 83 genes) and diterpenoid biosynthesis (map00904, 74 genes) of KEGG pathways. We speculate that these genes may be involved in regulating the synthesis of oridonin. Furthermore, 18 genes had a significant response to MeJA in the biosynthesis pathway of terpenoid compounds based on the genes mapped to terpenoid backbone biosynthesis (map00900, 83 genes) and the diterpenoid biosynthesis (map00904, 74 genes) of KEGG pathways. Interestingly, analysis of the diterpenoid pathway revealed that most genes of terpenoid backbone biosynthesis were up-regulated while more genes in the diterpenoid biosynthesis were down-regulated

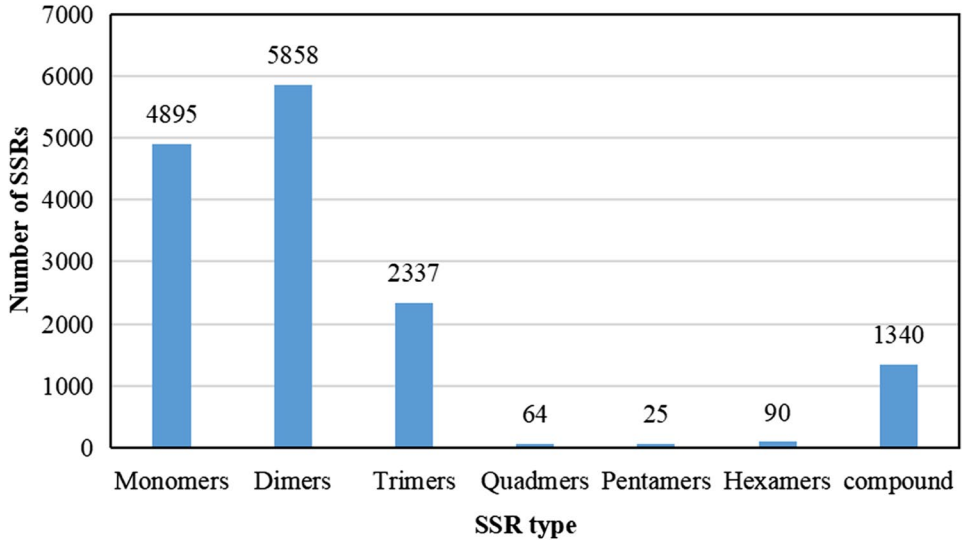


**Fig. 9** Statistics of the simple sequence repeats (SSRs) identified in *I. rubescens* transcriptome

(Table 3). These results suggested that MeJA can promote the increase of terpene backbone genes biosynthesis, and thus promote the synthesis of necessary substrates or initiators for terpenes. However, the composition of diterpenoids is complex, and the synthesis of different components of diterpenoids has substrate competition to some extent. Therefore, the expression of some genes in the diterpenoid synthesis pathway is decreased, while the expression of some corresponding components is increased.

Cytochrome P450 (CYP450) enzymes are known to play vital roles in plant evolution and metabolic diversification. They are especially essential to the biosynthesis of secondary metabolites in plants, such as lignins, terpenoids, sterols, fatty acids, hormones, pigments, and defense-related phytoalexins [32]. Previous studies have shown that some *CYP450* genes specifically regulate the synthesis of plant diterpenoids [33]. In our study, 10 *CYP450* genes were identified as possibly being involved in regulating the oridonin synthesis. Previous research has also shown that the *CYP450* genes involved in the biosynthesis of plant terpenoids are mainly attributed to the CYP51, CYP71, CYP72, CYP85, CYP86, CYP710, and CYP711 families [33]. In the study of *Taxus chinensis*, CYP450s play a major role in taxol biosynthesis. Approximately half of the 20 enzymatic steps of the pathway are thought to be catalyzed by CYP450 oxygenases [32, 34]. In tanshinone biosynthesis, *CYP76AH1* acts as the first CYP450 responsible for the production of oxygenated diterpenoid precursors [35]. In *Catharanthus roseus*, *CYP71D351* is involved in tabersonine 16-hydroxylase [36]. In addition, *CYP94B1*, *CYP94B2*, *CYP94B3*, and *CYP94C1* are responsible for catalyzing the terpenoid of sequential ω-oxidation of JA-Ile [37]. The above results indicate that cytochrome P450s are evolutionarily conserved enzymes involved in the catalysis of numerous reactions, especially in secondary metabolism.

In conclusion, multiple comparative transcriptome analyses were conducted to determine the differences in oridonin content in different lines of *I. rubescens* and to evaluate the induction effect of MeJA. The results of this experiment identified the differential genes responding to MeJA, and further screening of these genes revealed how they may regulate the oridonin synthesis. So, in the next stage of research, based on the results of this experiment, we will aim to use in *vitro* and in *vivo* verification technology (e.g., enzyme activity assays, gene overexpression, and gene silencing) to carry out functional verification analysis of related genes to strengthen the connection between these genes and oridonin biosynthesis. Overall, our work lays an important foundation for the complete analysis of the synthetic pathway of oridonin of *I. rubescens*.

## Conclusions

In this study, multiple comparative transcriptome analyses of JY (with oridonin) and LS (no oridonin) lines of *I. rubescens* with or without a methyl jasmonate (MeJA) treatment were conducted to determine the differences in oridonin content in different lines of *I. rubescens* and to evaluate the induction effect of MeJA. The results of this experiment identified the differential genes responding to MeJA, including transcription factors. And further screening of genes that there may regulate the oridonin synthesis. In addition, SNPs and SSRs were also detected in *I. rubescens*, providing further support for future genetic variation and marker-assisted selection. In conclusion, our work lays an important foundation for the complete analysis of the synthetic pathway of oridonin of *I. rubescens*.

## Materials and methods

### Plant materials and RNA extraction

The seeds of *I. rubescens* were collected from Jiyuan and LuShan of Henan Province, China. Then, the two lines of *I. rubescens* were grown in the same illumination incubator. At the Vegetative stage of plants (3 months after germination) which were grown in an illumination incubator with a relative humidity of 70%, a 16 h/8 h light/dark photoperiod (120 μmol $m^{-2}s^{-1}$), and a temperature of 24–26℃. The methyl jasmonate (MeJA) treatment consisted of a 200 μmol MeJA (Sigma Aldrich, St. Louis, MO, USA) aqueous solution which was evenly sprayed on the plant leaves. The leaves between three and six nodes were harvested at 0, 3, 6, 12, and 24 h after treatment. A portion of the collected samples were used to determine the content of oridonin and all remaining samples were immediately frozen in liquid nitrogen and preserved at − 80℃ for later analysis. For the plant material of *I. rubescens*, Prof. Suiqing Chen undertook the formal identification, and a voucher specimen (deposition number: 410881LY0045) of this material has been deposited in the herbarium of Medicinal Plants, Henan University of Chinese Medicine.

### Determination of oridonin in I. rubescens

Oridonin was extracted and detected according to the Pharmacopoeia of the People's Republic of China [7]. *I. rubescens* leaf samples were baked in an oven at 60 ℃ until a constant weight was achieved. A mortar was then used to grind the samples into a fine powder. 1 g of the resulting powder was placed in a conical flask and 50 mL of methanol was added. A stopper was used to seal the flask before being weighed. After resting for 30 min, a 30-minute ultrasonic treatment (power 250 W, frequency 40 kHz) was applied. Additional methanol was added to replace the weight lost during this treatment. The mixture was then shaken and filtered before 0.22 μm was obtained for testing. For the preparation of the control solution, an appropriate amount of oridonin reference solution was obtained and weighed. Methanol was then added to make a solution containing a concentration of 60 μg per 1 mL. 10 μL of both the control solution and the test solution were then independently added into a liquid chromatography setup for determination. The chromatographic conditions were as follows: Waters e2695/2998, Phenomenex C18 column (250 mm × 4.6 mm, 4 μm), moving phase methanol–water (55:45), detection wavelength 239 nm, flow rate 0.8 mL·$min^{-1}$, and column temperature 25 ℃.

### RNA extraction, cDNA library construction, and sequencing

Total RNA was extracted using Trizol reagent (Invitrogen, CA, USA) and following the manufacturer's procedure. The total RNA quantity and purity were analyzed by using a Bioanalyzer 2100 and RNA 1000 Nano LabChip Kit (Agilent, CA, USA) with RIN number > 7.0. Poly(A) RNA was purified from the total RNA (5ug) using poly-T oligo-attached magnetic beads and two rounds of purification. Following purification, the mRNA was fragmented into small pieces using divalent cations under an elevated temperature. The cleaved RNA fragments were then reverse-transcribed to create the final cDNA library following the protocol for the mRNA-Seq sample preparation kit (Illumina, San Diego, USA). The average insert size for the paired-end libraries was 300 bp (± 50 bp). Paired-end sequencing was then performed using an Illumina Novaseq™ 6000 (LC Sciences, USA) following the vendor's recommended protocol.

### Transcriptome data assembly and unigene annotation

The raw reads with adaptor and poly-N sequences and low-quality reads (Q-value < 10 in more than 50% of the bases) were removed by Cutadapt [38] and Perl scripts in-house. FastQC (http://www.bioinformatics.babraham.ac.uk/projects/fastqc/) was used to verify sequence quality and propertied including the Q20, Q30, and GC-content of the clean data. All downstream analyses were based on clean and high-quality data. Transcriptome assembly was conducted using Trinity 2.4.0 software with the minimum K-mer value set to 1 [39]. The longest transcript in each cluster was chosen as the 'gene' sequence (aka Unigene). For the unigene annotation, all assembled unigenes were aligned against the non-redundant (Nr) protein database (http://www.ncbi.nlm.nih.gov/), Gene ontology (GO) (http://www.geneontology.org), SwissProt (http://www.expasy.ch/sprot/), Kyoto Encyclopedia of Genes and Genomes (KEGG) (http://www.genome.jp/kegg/), and eggNOG (http://eggnogdb.embl.de/) databases using DIAMOND [40] with a threshold of Evalue < 0.00001. PlantTFDB (http://planttfdb.gao-lab.org/) was used for identification and classification of TFs based on the reference of *Salvia miltiorrhiza* transcription factors by using BLASTX with an E-value cutoff $1e^{-6}$ and according to the domains presence in InterPro. A microsatellite program (MISA) (http://pgrc.ipk-gatersleben.de/misa/) was used to SSRs identification in the transcriptome.

### Differentially expressed unigene analysis

The quantification expression levels for unigenes were calculated by Salmon [41] using TPM (Transcripts Per Million reads) [42]. The differentially expressed unigenes (DEGs)with $\log_2$ (fold change) > 1 or $\log_2$ (fold change) < −1 and statistical significance (p-value < 0.05) were selected by R package edgeR [43]. Heatmap was made by advanced heatmap tool in OmicStudio Platform (https://www.omicstudio.cn/tool) [44].

### RT-qPCR validation

To confirm the results of high-throughput sequencing, twelve unigenes were randomly selected for RT-qPCR analysis between different treatments. The total RNA of each *I. rubescens* sample was reverse-transcribed using the BCS HIScriptTM AII-in-One Mix with dsDNA. This kit was used to remove genomic DNA contamination and to synthesize the first strand of cDNA via reverse transcription. The obtained cDNA was adjusted to the corresponding concentration based on quantification with the ultramicro spectrophotometer before being stored at − 20 °C for further use. The cDNA of *I. rubescens* samples were used as templates and *eIF* gene was used as the internal reference gene for RT-qPCR [45]. The reaction system was as follows: 10 μL of 2 × TransStart® Top Green qPCR SuperMix, 0.4 μL of 50 × Passive Reference Dye II, 0.4 μL of both forward and reverse primers (10 μM), 2 μL of sample cDNA, and 6.8 μL $ddH_2O$. 45 reaction cycles were completed under the following conditions: 94 °C 30 s, 94 °C 5 s, and 60 °C 30 s. Each RT-qPCR was performed with three biological replicates and three technical repetitions. The relative expression of genes was calculated by the $2^{-\Delta\Delta Ct}$ method [46]. The primers for RT-qPCR are included in Table S1.

## Supplementary Information

The online version contains supplementary material available at https://doi.org/10.1186/s12870-025-07460-3.

Supplementary Material 1.

#### Acknowledgements

The author thanks LC-bio for its support of RNA-seq services.

#### Authors' contributions

C.L. and S.C. conceived and designed the research framework; F.Z., B.Z., J.L. and J.Y. prepared the sample and performed the experiments; C.L., F.Z., H.Y., and J.L. analyzed the data; C.L. and B.Z. wrote the paper; C.L., B.Z., and S.C. made revisions to the final manuscript; C.L. and S.C.; funding acquisition. All authors have read and approved the final manuscript.

#### Funding

This research was supported by the National Natural Science Foundation of China (82574543), the Natural Science Foundation of Henan (232301420078), the Henan Province Chinese herbal medicine industry technology system (No.14 [2018]), and the Fourth National Traditional Chinese Medicine Resource Survey Project (No.40 [2019]).

#### Data availability

The all raw data presented in this study have been deposited in the Sequence Read Archive (SRA) to NCBI under BioProject accession number PRJNA910296.

## Declarations

#### Ethics approval and consent to participate

There is no ethics approval and consent to participate in this manuscript. During the experiment, no specific permits were required for the described field studies, all plant materials were used in accordance with national and international standards and local laws and regulations. The use of all plant materials does not pose any risk to other species in nature. The collection of germplasm and planting area of *Isodon rubescens* samples does not involve endangered or protected species. All *Isodon rubescens* samples were stored in Henan University of Chinese Medicine. These samples materials can be accessed at the request of the corresponding author.

#### Consent for publication

Not applicable.

#### Competing interests

The authors declare no competing interests.

Received: 15 February 2023 / Accepted: 19 September 2025
Published online: 17 October 2025

#### References

1. Zhang W, Huang Q, Hua Z-C. Oridonin: A promising anticancer drug from China. Front Biology. 2010;5(6):540–5.
2. Pi J, Cai H, Jin H, Yang F, Jiang J, Wu A, Zhu H, Liu J, Su X, Yang P, et al. Qualitative and quantitative analysis of ROS-Mediated Oridonin-Induced oesophageal cancer KYSE-150 cell apoptosis by atomic force microscopy. PLoS ONE. 2015;10(10):e0140935.
3. Yang J, Ren X, Zhang L, Li Y, Cheng B, Xia J. Oridonin inhibits oral cancer growth and PI3K/Akt signaling pathway. Biomed Pharmacother. 2018;100:226–32.
4. Liu QQ, Chen K, Ye Q, Jiang XH, Sun YW. Oridonin inhibits pancreatic cancer cell migration and epithelial-mesenchymal transition by suppressing Wnt/beta-catenin signaling pathway. Cancer Cell Int. 2016;16:57.
5. Li D, Han T, Xu S, Zhou T, Tian K, Hu X, Cheng K, Li Z, Hua H, Xu J. Antitumor and antibacterial derivatives of oridonin: A main composition of Dong-Ling-Cao. Molecules. 2016;21(5):575.
6. He F, Bai YH, Wang J, Wei J, Yu CY, Li S, Yang WL, Han CH. Isolation and purification of Oridonin from the whole plant of *Isodon rubescens* by High-Speed Counter-Current chromatography. Molecules. 2011;16(9):7949–57.
7. Committee NP. Pharmacopoeia of the people's Republic of China. Beijing, China: Chinese Medical Science and Technology; 2020.
8. Vranova E, Coman D, Gruissem W. Network analysis of the MVA and MEP pathways for isoprenoid synthesis. Annu Rev Plant Biol. 2013;64:665–700.
9. Bergman ME, Davis B, Phillips MA. Medically useful plant terpenoids: Biosynthesis, Occurrence, and mechanism of action. Molecules. 2019;24(21):3961.
10. Guo J, Ma Y. Biosynthetic Pathway of Tanshinones in Salvia miltiorrhiza. In: The Salvia miltiorrhiza Genome. Edited by Lu S. Cham: Springer International Publishing; 2019. p. 129–139.
11. Akhila A, Rani K, Thakur RS. Biosynthesis of Artemisinic acid in Artemisia annua. Phytochemistry. 1990;29(7):2129–32.
12. Yu CN, Zhang CC, Xu XY, Huang JF, Chen YY, Luo XJ, Wang HZ, Shen CJ. Omic analysis of the endangered Taxaceae species Pseudotaxus chienii revealed the differences in taxol biosynthesis pathway between Pseudotaxus and taxus yunnanensis trees. BMC Plant Biol. 2021;21(1):104.
13. Jin BL, Cui GH, Guo J, Tang JF, Duan LX, Lin HX, Shen Y, Chen T, Zhang HB, Huang LQ. Functional diversification of Kaurene Synthase-Like genes in Isodon rubescens. Plant Physiol. 2017;174(2):943–55.
14. Sun YW, Shao J, Liu HL, Wang H, Wang GY, Li JH, Mao YP, Chen Z, Ma K, Xu L, et al. A chromosome-level genome assembly reveals that tandem-duplicated CYP706V oxidase genes control Oridonin biosynthesis in the shoot apex of Isodon rubescens. Mol Plant. 2023;16(3):517–32.
15. Yin XY, Yan X, Qian CJ, Zhou SS, Fang TZ, Fan XK, Gao Y, Chang YX, Yang J, Ma XF. Comparative transcriptome analysis to identify genes involved in terpenoid biosynthesis in agriophyllum squarrosum, a folk medicinal herb native to Asian temperature deserts. Plant Biotechnol Rep. 2021;15(3):369–87.
16. Mazzoni-Putman SM, Brumos J, Zhao C, Alonso JM, Stepanova AN. Auxin interactions with other hormones in plant development. Cold Spring Harb Perspect Biol. 2021;13(10):a039990.
17. Wasternack C. Jasmonates: an update on biosynthesis, signal transduction and action in plant stress response, growth and development. Ann Bot. 2007;100(4):681–97.
18. Rui Z, Xiu-Juan W, Wei G. [Regulation mechanism of plant hormones on secondary metabolites]. Zhongguo Zhong Yao Za Zhi. 2020;45(17):4205–10.
19. De Geyter N, Gholami A, Goormachtig S, Goossens A. Transcriptional machineries in jasmonate-elicited plant secondary metabolism. Trends Plant Sci. 2012;17(6):349–59.

20. Lin T, Du J, Zheng X, Zhou P, Li P, Lu X. Comparative transcriptome analysis of MeJA-responsive AP2/ERF transcription factors involved in notoginsenosides biosynthesis. 3 Biotech. 2020;10(7):290.
21. Lackman P, Gonzalez-Guzman M, Tilleman S, Carqueijeiro I, Perez AC, Moses T, Seo M, Kanno Y, Hakkinen ST, Van Montagu MC, et al. Jasmonate signaling involves the abscisic acid receptor PYL4 to regulate metabolic reprogramming in Arabidopsis and tobacco. Proc Natl Acad Sci U S A. 2011;108(14):5891–6.
22. Banerjee S, Roy P, Roy S. Transcription Factor Mediated Plant Metabolite Production in Response to Environmental Stress Factors: Current Understanding and Future Aspects. In: Metabolic Engineering in Plants. Edited by Aftab T, Hakeem KR. Singapore: Springer Nature Singapore; 2022. p. 91–122.
23. Ganal MW, Altmann T, Roder MS. SNP identification in crop plants. Curr Opin Plant Biol. 2009;12(2):211–7.
24. Duarte J, Riviere N, Baranger A, Aubert G, Burstin J, Cornet L, Lavaud C, Lejeune-Henaut I, Martinant JP, Pichon JP, et al. Transcriptome sequencing for high throughput SNP development and genetic mapping in pea. BMC Genomics. 2014;15:126.
25. Wang L-Y, Li S-S, Wang T-Y, He C-Y, Luo H-M, Zhang J-G, Zeng Y-F. Genomic SSR and EST-SSR markers for phylogenetic and pedigree reconstructions—A comparison in sea Buckthorn. Plant Breeding. 2021;140(1):167–83.
26. Li Y, Lin Y, Jia B, Chen G, Shi H, Xu R, Li X, Tang J, Tang Q, Zhang G, et al. Transcriptome analysis reveals molecular mechanisms underlying Methyl Jasmonate-mediated biosynthesis of Protopanaxadiol-type saponins in Panax Notoginseng leaves. J Plant Biology. 2022;65(1):29–41.
27. Luo M, Zhou X, Hao Y, Sun H, Zhou Q, Sun Y, Ji S. -j: Methyl jasmonate pretreatment improves aroma quality of cold-stored 'Nanguo' Pears by promoting ester biosynthesis. Food Chem. 2021;338:127846.
28. Ee S-F, Oh J-M, Mohd Noor N, Kwon T-R, Mohamed-Hussein Z-A, Ismail I, Zainal Z. Transcriptome profiling of genes induced by Salicylic acid and Methyl jasmonate in polygonum minus. Mol Biol Rep. 2013;40(3):2231–41.
29. Sun YZ, Niu YY, Xu J, Li Y, Luo HM, Zhu YJ, Liu MZ, Wu Q, Song JY, Sun C, et al. Discovery of WRKY transcription factors through transcriptome analysis and characterization of a novel Methyl jasmonate-inducible PqWRKY1 gene from Panax Quinquefolius. Plant Cell Tiss Org. 2013;114(2):269–77.
30. Kim OT, Um Y, Jin ML, Kim YC, Bang KH, Hyun DY, Lee HS, Lee Y. Analysis of expressed sequence tags from centella Asiatica (L.) urban hairy roots elicited by Methyl jasmonate to discover genes related to cytochrome P450s and glucosyltransferases. Plant Biotechnol Rep. 2014;8(2):211–20.
31. Ge Q, Xiao YP, Wang ZZ. Cloning and characterization of a MeJA-responsive jasmonate ZIM-domain gene (SmJAZ1) from salvia miltiorrhiza bunge. Russ J Plant Physl. 2014;61(6):862–72.
32. Rasool S, Mohamed R. Plant cytochrome P450s: nomenclature and involvement in natural product biosynthesis. Protoplasma. 2016;253(5):1197–209.
33. Zheng X, Li P, Lu X. Research advances in cytochrome P450-catalysed pharmaceutical terpenoid biosynthesis in plants. J Exp Bot. 2019;70(18):4619–30.
34. Liao W, Zhao S, Zhang M, Dong K, Chen Y, Fu C, Yu L. Transcriptome assembly and systematic identification of novel cytochrome P450s in taxus chinensis. Front Plant Sci. 2017;8:1468.
35. Guo J, Zhou YJ, Hillwig ML, Shen Y, Yang L, Wang Y, Zhang X, Liu W, Peters RJ, Chen X, et al. CYP76AH1 catalyzes turnover of miltiradiene in Tanshinones biosynthesis and enables heterologous production of ferruginol in yeasts. Proc Natl Acad Sci USA. 2013;110(29):12108–13.
36. Carqueijeiro I, Brown S, Chung K, Dang TT, Walia M, Besseau S, Duge de Bernonville T, Oudin A, Lanoue A, Billet K, et al. Two Tabersonine 6,7-Epoxidases initiate Lochnericine-Derived alkaloid biosynthesis in catharanthus roseus. Plant Physiol. 2018;177(4):1473–86.
37. Bruckhoff V, Haroth S, Feussner K, Konig S, Brodhun F, Feussner I. Functional characterization of CYP94-Genes and identification of a novel jasmonate catabolite in flowers. PLoS ONE. 2016;11(7):e0159875.
38. Martin M. Cutadapt removes adapter sequences from high-throughput sequencing reads. EMBnet J. 2011;17(1):10–2.
39. Grabherr MG, Haas BJ, Yassour M, Levin JZ, Thompson DA, Amit I, Adiconis X, Fan L, Raychowdhury R, Zeng QD, et al. Full-length transcriptome assembly from RNA-Seq data without a reference genome. Nat Biotechnol. 2011;29(7):644–52.
40. 38, Buchfink B, Xie C, Huson DH. Fast and sensitive protein alignment using DIAMOND. Nat Methods. 2015;12(1):59–60.
41. Patro R, Duggal G, Love MI, Irizarry RA, Kingsford C. Salmon provides fast and bias-aware quantification of transcript expression. Nat Methods. 2017;14(4):417–9.
42. Mortazavi A, Williams BA, Mccue K, Schaeffer L, Wold B. Mapping and quantifying mammalian transcriptomes by RNA-Seq. Nat Methods. 2008;5(7):621–8.
43. Robinson MD, McCarthy DJ, Smyth GK. EdgeR: a bioconductor package for differential expression analysis of digital gene expression data. Bioinformatics. 2010;26(1):139–40.
44. Lyu F, Han F, Ge C, Mao W, Chen L, Hu H, Chen G, Lang Q, Fang C. OmicStudio: A composable bioinformatics cloud platform with real-time feedback that can generate high-quality graphs for publication. iMeta. 2023;2(1):e85.
45. Lian CL, Zhang B, Yang JF, Lan JX, Yang H, Guo KH, Li JJ, Chen SQ. Validation of suitable reference genes by various algorithms for gene expression analysis in Isodon rubescens under different abiotic stresses. Sci Rep-Uk. 2022;12(1):19599.
46. Livak KJ, Schmittgen TD. Analysis of relative gene expression data using real-time quantitative PCR and the 2(-Delta delta C(T)) method. Methods. 2001;25(4):402–8.


## Publisher's Note